Electronic Supplementary Material (ESI) for Nanoscale.

Supporting Information

Broadband Plasmonic Indium Arsenide Photonic Antennas

*Xinghui Liu[1,2], Mengfei Xue[3,1,2], and Jianing Chen[1,2,4 *]*

[1] Beijing National Laboratory for Condensed Matter Physics, Institute of Physics, Chinese Academy of Sciences, Beijing 100190, China

[2] School of Physical Sciences, University of Chinese Academy of Sciences, Beijing 100049, China

[3] Wenzhou Institute, University of Chinese Academy of Sciences, Wenzhou, Zhejiang 325001, China

[4] Songshan Lake Materials Laboratory, Dongguan, Guangdong 523808, China

*E-mail: jnchen@iphy.ac.cn

Fig. S1 shows electromagnetic field enhancement at the metallic tip apex[1]. The 10 μm laser incident at 30˚ to the positive *x* direction. The radius of the tip apex is 20 nm. **Fig. S1a** shows the field enhancement is about 8 at the tip apex when the angle between the incident laser's polarization direction and the positive *x* direction is 60˚. **Fig. S1b** shows no field enhancement at the tip apex when the incident laser's polarization direction is parallel to the *y*-axis. Fig. S1c show the field enhancement versus the incident wavelength when the incident laser's polarization direction is parallel to the tip's axis.

Fig. S2 shows nano-images of different InAs twinning superlattice (TSL) nanowire Fabry-Perot (F-P) plasmonic resonance modes. Experiment results of m = 2 (**Fig. S2a**), 3 (**Fig. S2b**) for NW-S and m = 4 (**Fig. S2c**), 5 (**Fig. S2d**), 6 (**Fig. S2e**) for NW-L are demonstrated. The order of resonance modes m = n + 1, n is the number of standing wave fringes excluding the bright spots at both ends. Employing COMSOL 5.2a, we simulated InAs TSL nanowire's surface electrical field at the resonance frequency of these modes for NW-S (**Fig. S2f-g**) and NW-L (**Fig. S2h-j**). In all simulations, the metallic tip was modeled by a vertically oriented point dipole source. To avoid the influence of the dipole electric field on the recorded signal, we set the point dipolar 300 nm above the nanowire and record the vertical component of the electric field E_z 20 nm above the nanowire[2]. The nano-images were obtained by scanning the point dipolar parallel to the substrate with 10 nm step sizes at a fixed excitation frequency. The nano-FTIR spectra were obtained by changing the excitation frequency when the point dipolar at a fixed position. The hyperspectral images were obtained by repeating spectral manipulation along the nanowire's long axis with 10 nm step sizes. The permittivity of InAs nanowire was given by the Drude model $\varepsilon(\omega) = \varepsilon_\infty\left(1 - \frac{\omega_p^2}{\omega^2+i\omega\gamma}\right)$, where ε_∞ is background permittivity, ω is angular frequency, γ is the scattering rate, and ω_p is plasma frequency which can be written as $\omega_p = \sqrt{\frac{ne^2}{m^*\varepsilon_0\varepsilon_\infty}}$, where ε_0 is the vacuum permittivity, e is elementary charge, n is the carrier density, m^* is the carrier effective mass. In the simulation, γ^{-1} = 0.1 ps, ε_∞ = 11.8, and $m^* = 0.023m_e$ are taken from previous reports[3]. The dielectric functions of SiO_2 is taken from previous reports[4].

Fig. S3 demonstrates the schematic of the plasmons launched by the tip propagating along the nanowire's axis and reflected by the nanowire ends. In **Fig. S3a**, the plasmons cannot propagate more than two trips along the nanowire axis for a long nanowire. In this case, the electric field below the tip is formed by the interference between the tip-launched plasmons and the first reflected plasmons. In **Fig. S3b**, the plasmons can propagate more than two trips along the nanowire axis for a short nanowire. In this case, the electric field below the tip is formed by the interference between the tip-launched plasmons, the first reflected plasmons, and the second reflected plasmons. As the number of reflections increases, the loss caused by reflection must be considered.

Fig. S4 demonstrates the *Q* factor calculation of NW-L's different F-P modes. Experimental results (red dots) and fitting lines (black line) profiles of m = 3 (**Fig. S4a**), 4 (**Fig.

S4d), 5 (**Fig. S4g**), 6 (**Fig. S4j**), 7 (**Fig. S4m**) modes. The standing wave pattern of the surface plasmons can be treated as two sinusoidal damping waves launched from the nanowire ends (wave I launched from the right end; wave II launched from the left end). **Fig. S4b, e, h, k, n** shows wave I and wave II of mode m = 3 – 7 in the assumption R = 0.1, respectively. In this case, the intensity of wave I (II) is small enough to be ignored after being reflected at the left (right) end. **Fig. S4c, f, i, l, o** shows wave I and wave II of mode m = 3 – 7 in the assumption R = 1, respectively. In this case, the intensity of wave I (II) is large enough after being reflected at the left (right) end.

Fig. S5 demonstrates the *Q* factor for NW-T plasmons in simulation at $\omega = 990\ cm^{-1}$, $950\ cm^{-1}$, $900\ cm^{-1}$, $760\ cm^{-1}$, $670\ cm^{-1}$. NW-T is 10 μm in length and 210 nm in diameter (diameter is similar to NW-L). The red dot lines are obtained by scanning the point dipolar along the nanowire's long axis with 10 nm step sizes at the fixed excitation frequency. The excitation frequency is fixed at $670\ cm^{-1}$, $760\ cm^{-1}$, $900\ cm^{-1}$,$950\ cm^{-1}$, $990\ cm^{-1}$ for m = 3, 4, 5, 6, 7 modes of NW-L, respectively. The black lines are fitting line profiles using the function[5]:

$$F = e^{-\frac{2\pi x}{(Q\lambda_p)}} sin\frac{4\pi x}{\lambda_p}$$

The *Q* factor of NW-T is 5.89, 7.11, 7.35, 6.67, 4.72 at $\omega = 670\ cm^{-1}$, $760\ cm^{-1}$, $900\ cm^{-1}$,$950\ cm^{-1}$, $990\ cm^{-1}$, respectively.

Fig. S6 demonstrates the relationship of the *Q* factor with the nanowire's diameter and excitation frequency. The data are derived from the simulation of a 10 μm long nanowire. **Fig. S6a** shows the *Q* factor when the nanowire's diameter is 50 – 225 nm at $\omega = 930\ cm^{-1}$. **Fig. S6b** shows the *Q* factor when the excitation frequency is 860 – $1000\ cm^{-1}$ with the 125 nm in nanowire's diameter. As the nanowire's diameter or excitation frequency decreases, the *Q* factor decreases from 10 to 5.

FIGURES

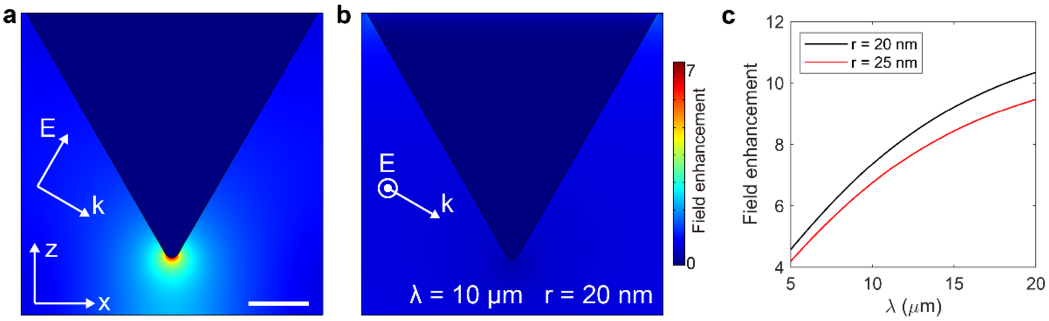

Fig. S1 Electromagnetic field enhancement of metallic tip when the incident laser's polarization direction is parallel (a) and perpendicular (b) to the tip's axis. (c) Field enhancement is compared to the incident wavelength when the laser's polarization direction is parallel to the tip's axis.

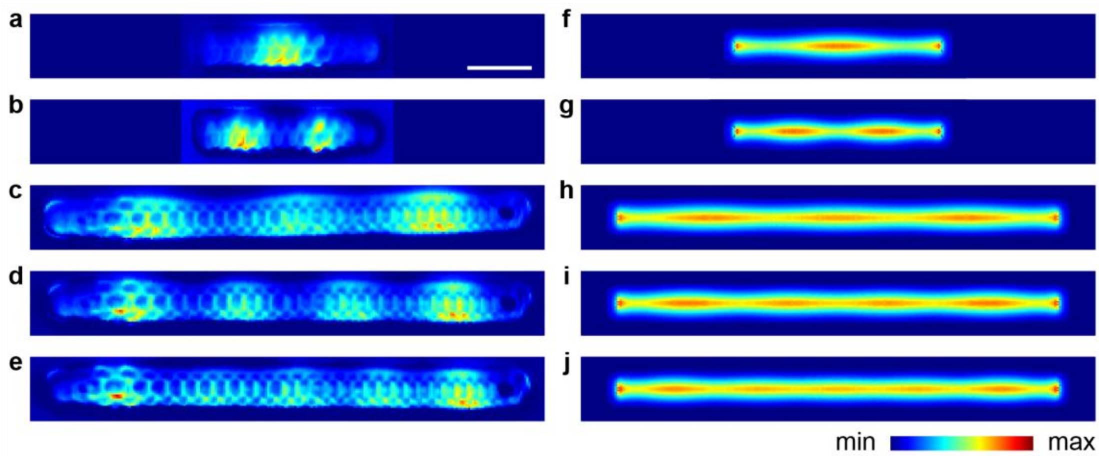

Fig. S2 Nano-imaging of different InAs twinning superlattice nanowire (TSL) Fabry-Perot (F-P) plasmonic resonance modes derived by experiment (a-e) and simulation (f-j).

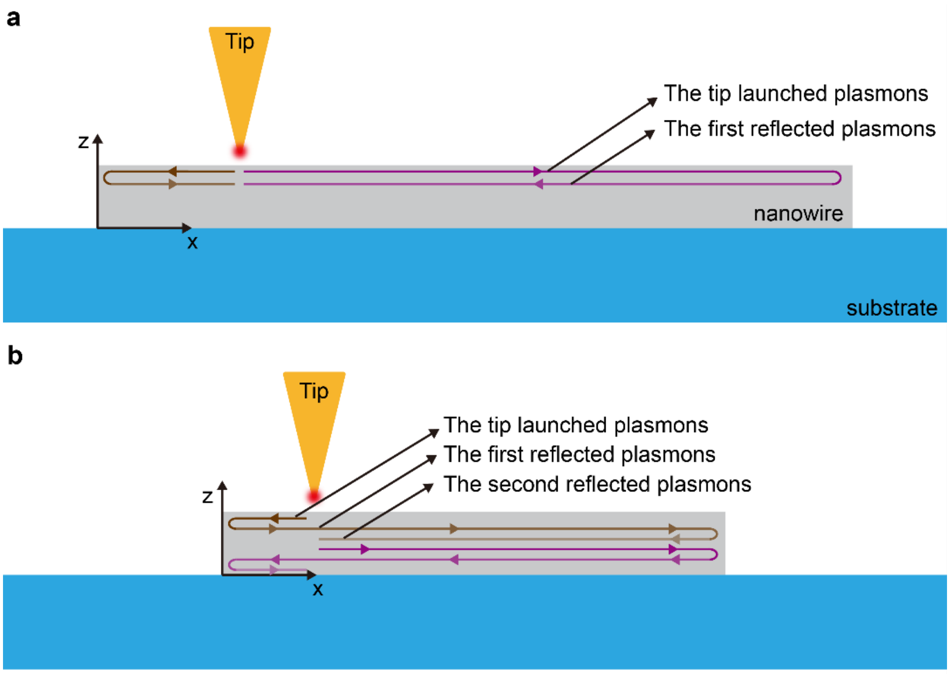

Fig. S3 Schematic of the plasmons launched by the tip propagate along a long (a) and short (b) nanowire's axis.

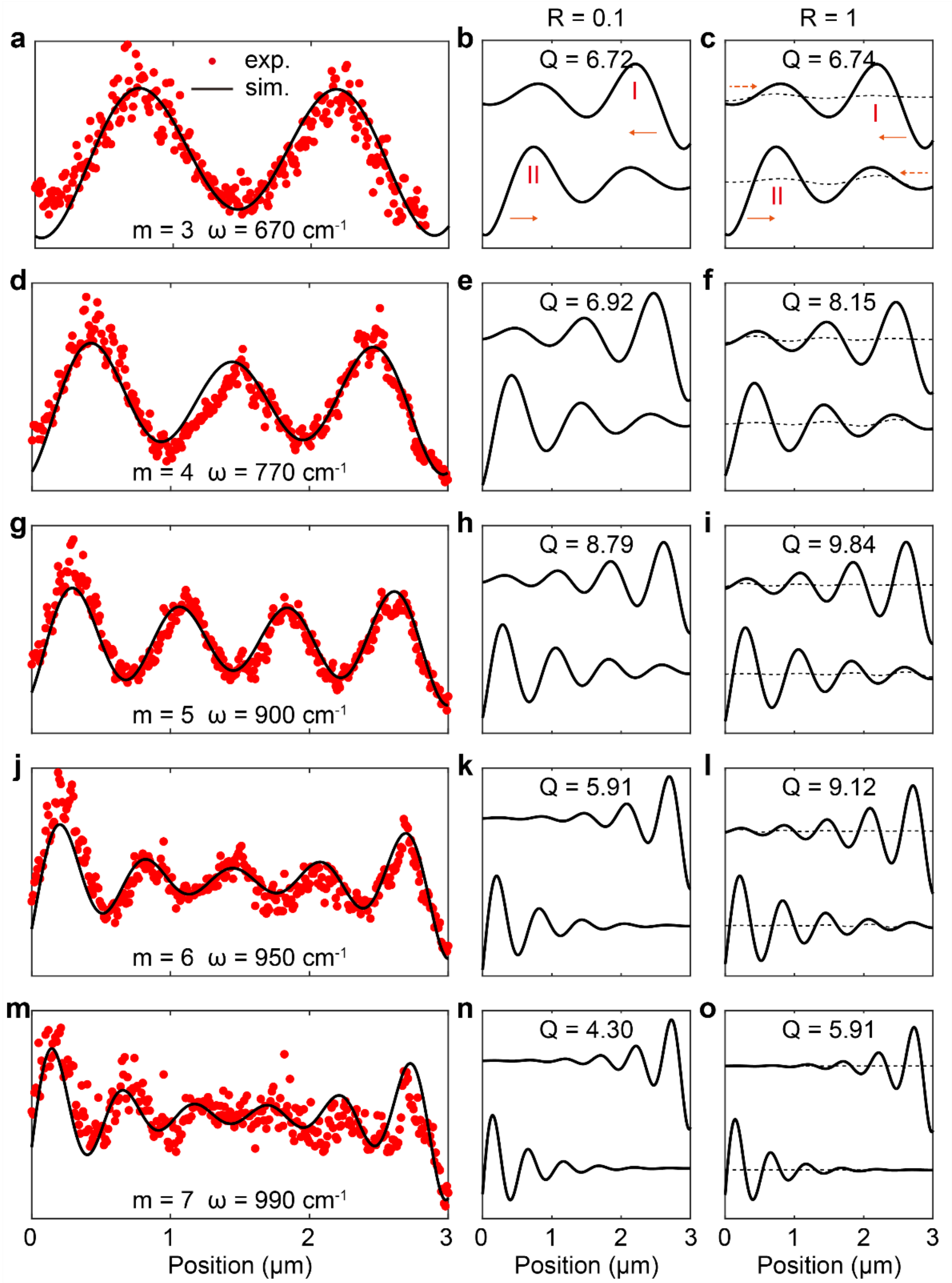

Fig. S4 The Q factor calculation of m=3 (a-c),4 (d-f), 5 (g-i), 6 (j-l), 7 (m-o) modes for NW-L.

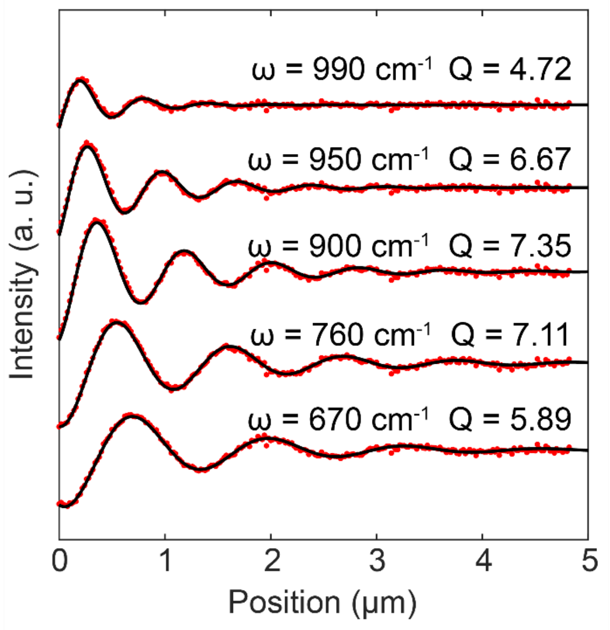

Fig. S5 The Q factor for the plasmons of NW-T in simulation at ω = 990cm^{-1}, 950cm^{-1}, 900cm^{-1}, 760cm^{-1}, and 670cm^{-1}.

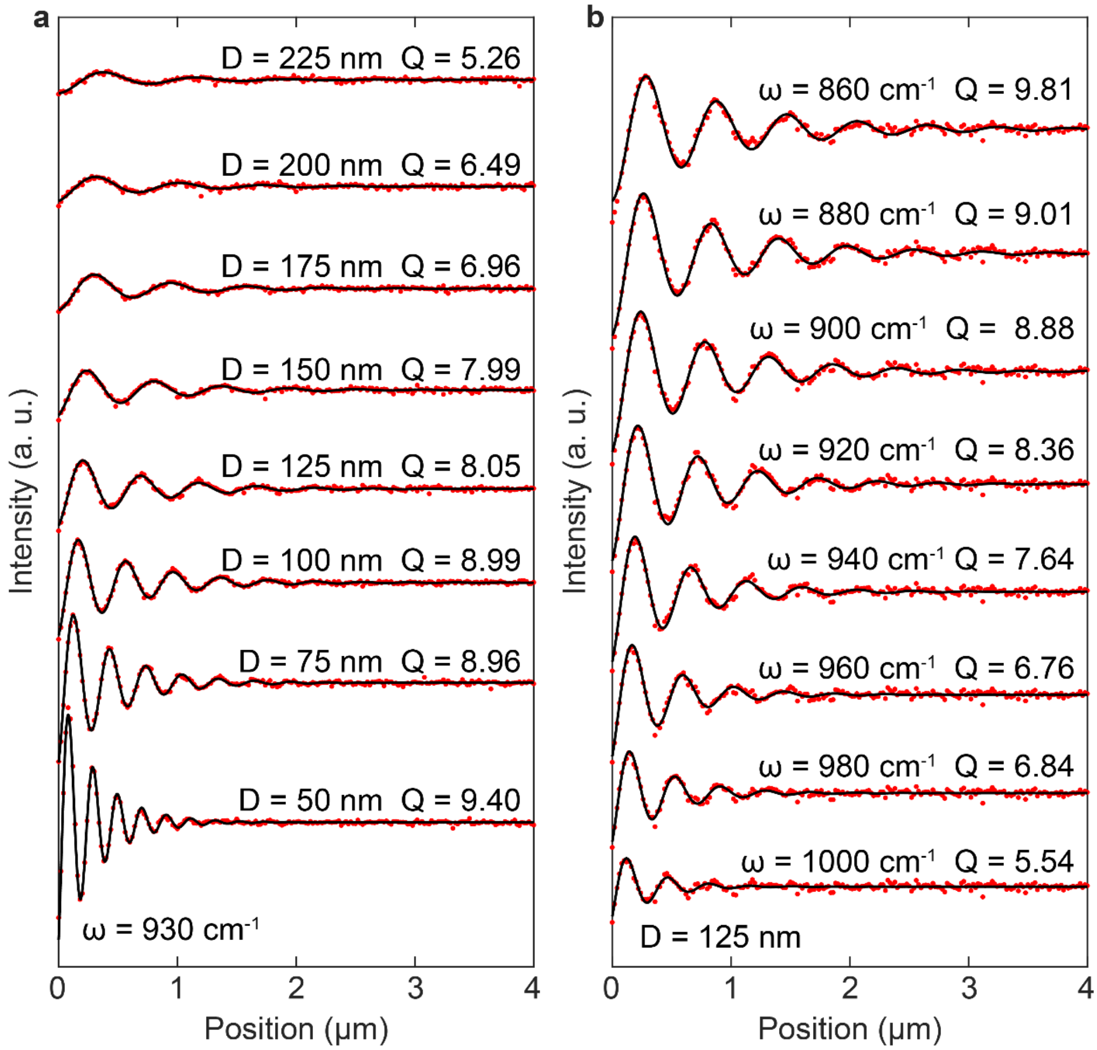

Fig. S6 The relationship of the *Q* factor with the nanowire's diameter (a) and excitation frequency (b). The red dot lines are simulated results, and the black lines are fitting profiles.

REFERENCES

1. A. J. Huber, F. Keilamnn, J. Wittborn, J. Aizpurua and R. Hillenbrand, *Nano Letters*, 2008, **8**, 3766-3770.
2. F. J. Alfaro-Mozaz, P. Alonso-González, S. Vélez, I. Dolado, M. Autore, S. Mastel, F. Casanova, L. E. Hueso, P. Li, A. Y. Nikitin and R. Hillenbrand, *Nature Communications*, 2017, **8**, 15624.
3. D. V. Seletskiy, M. P. Hasselbeck, J. G. Cederberg, A. Katzenmeyer, M. E. Toimil-Molares, F. Léonard, A. A. Talin and M. Sheik-Bahae, *Physical Review B*, 2011, **84**, 115421.
4. Z. Fei, G. O. Andreev, W. Bao, L. M. Zhang, A. S McLeod, C. Wang, M. K. Stewart, Z. Zhao, G. Dominguez, M. Thiemens, M. M. Fogler, M. J. Tauber, A. H. Castro-Neto, C. N. Lau, F. Keilmann and D. N. Basov, *Nano Letters*, 2011, **11**, 4701-4705.
5. Z. Shi, X. Hong, H. A. Bechtel, B. Zeng, M. C. Martin, K. Watanabe, T. Taniguchi, Y.-R. Shen and F. Wang, *Nature Photonics*, 2015, **9**, 515–519.